JMST Advances (2020) 2:77–88
https://doi.org/10.1007/s42791-020-00032-6

Online ISSN 2524-7913
Print ISSN 2524-7905

REVIEW

Architecture and mass transport properties of graphene-based membranes

Heechan Yang[1] · Jonghyun Baek[1] · Hyung Gyu Park[1]

Received: 13 May 2020 / Revised: 13 May 2020 / Accepted: 18 June 2020 / Published online: 20 August 2020

Abstract

A recently rising question of the applicability of two-dimensional (2D) materials to membranes of enhanced performance in water technology is drawing attention increasingly. At the center of the attention lies graphene, an atom-thick 2D material, for its readiness and manufacturability. This review presents an overview of recent research activities focused on the fundamental mass transport phenomena of two feasible membrane architectures from graphene. If one could perforate pores in a pristine impermeable graphene sheet with dimensional accuracy, the perforated 2D orifice would show unrivaled permeation of gases and liquids due to the 0D atomic barrier. If possibly endowed with selectivity, the porous graphene orifice would avail potentially for membrane separation processes. For example, it is noteworthy that results of molecular dynamics simulations and several early experiments have exhibited the potential use of the ultrathin permeable graphene layer having sub-nanometer-sized pores for a water desalination membrane. The other membrane design is obtainable by random stacking of moderately oxidized graphene platelets. This lamellar architecture suggests the possibility of water treatment and desalination membranes because of subnanometric interlayer spacing between two adjacent graphene sheets. The unique structure and mass transport phenomena could enlist these graphene membrane architectures as extraordinary membrane material effective to various applications of membrane technology including water treatment.

Graphic abstract

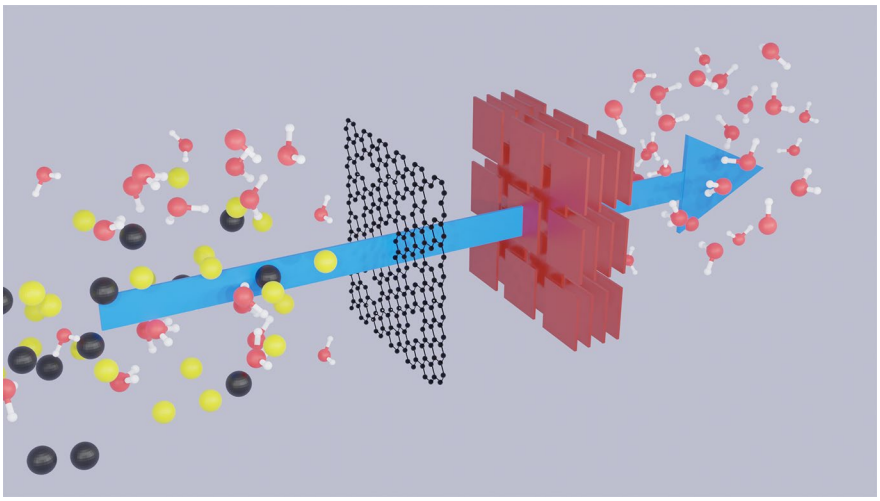

Keywords Two-dimensional materials · Graphene · Perforated 2D orifice · Oxidized graphene platelets · Lamellar architecture · Unrivaled permeation · Selectivity · Membrane separation processes · Water treatment

✉ Hyung Gyu Park
iduserpark@gmail.com

Extended author information available on the last page of the article

1 Introduction

The rise of atomically thin graphene is allowing a new study of the material and exploration of new device designs of membrane technology. Because of the two-dimensional (2D) nature of the sp^2-hybridized hexagonal carbon crystal [1], graphene exhibits outstanding material strength, such as incomparable stiffness and high fracture strength [2], leading to widespan studies from solid-state physics to fluid mechanics, mass transfer and membrane technology. In particular, the ultra thinness of the material represents its potential in separation technology. Also, a layer-by-layer stacking design of graphene and graphene oxide finds its use in selectivity control.

2 Graphene as a mass transport barrier

One of the most important features of graphene is a strong diffusion barrier. Intact single-crystalline graphene lattice has been found impermeable to most gas species including H_2 and He, at ambient conditions [2–4]. Considering the magnitude of the energy barrier (~1.3 eV < 3.2 eV < 4.2 eV < 5.5 eV) predicted by density functional theory, selective atomic permeation is likely to occur between B, N, H, and O, and the potential for B to pass through pristine graphene could be made through a complex process of coupling conversion caused by heat treatment, for example [5]. Therefore, at room temperatures, the lattice structure of two-dimensional carbon crystals would not allow any gas passage, thereby functioning as an effective mass transfer barrier [6]. However, molecular dynamics and experiments are indicating that particles as small as proton or order-of-magnitude more energetic than the room-temperature thermal energy may possibly penetrate the graphene lattice without causing considerable damage [7, 8].

Due to its excellent properties, graphene is used for corrosion protection coatings. Indeed, several research studies have demonstrated that the monocrystalline graphene layer can effectively prevent corrosion of the coated substrate [9, 10]. For large area and polycrystalline graphene coating, on the other hand, corrosion occurs owing to grain boundaries and lattice defects that can facilitate penetration of water and gases [11, 12]. Local corrosion damage [13] at the grain boundaries can be prevented by patching them with atomic layer deposition [10] or by coating graphene in multiple layers.

3 Membrane permeation theory

In view of membrane technology, the molecular impermeability lends atomically thin graphene conceptual eligibility for a selective membrane. Mass transport across the graphene layer will occur mainly through defects or artificial perforations in the graphene crystal. The transport resistance of a conventional manifold filter with thickness, l, is determined by the wall friction associated with viscosity inside the channel, and the relationship between flow resistance and mass transport rate, Q, is modeled as the classical Hagen–Poiseuille flow, i.e., solution of Navier–Stokes equation from continuum mechanics: $Q \propto l^{-1}$. However, when the friction mechanisms of channel walls disappear, the flow resistance involved in mass transport would be minimized. As a fluid with a dynamic viscosity, μ, crosses an extremely thin orifice with radius, r, driven by a differential pressure Δp, the dominant resistance to the flow would be an entrance effect. Sampson found a theoretical solution of Stokes flow through a single orifice [14], and later Tio and coworkers extended this solution by introducing porosity, κ, and constants ($S_3 = 9.03362$, $S_5 = 5.09026$, $S_7 = 4.42312$, $S_9 = 4.19127$) for an array of perforations in an infinitely thin disk [15].

$$Q_{\text{Sampson}} = \frac{r^3}{3\mu}\Delta p\left(1 - \frac{2S_3}{3\pi^{5/2}}\kappa^{3/2} - \frac{6S_5}{5\pi^{7/2}}\kappa^{5/2} - \frac{18S_7}{7\pi^{9/2}}\kappa^{7/2} - \frac{56S_9}{9\pi^{11/2}}\kappa^{9/2}\ldots\right)^{-1}.$$

Entrance resistance is always effective at any perforation and yet is often neglected if the flow resistance caused by viscous interactions inside the channel is dominant, e.g., where the membrane's internal pores are channels of finite length. However, for atomically thin membranes, the entrance resistance should be considered.

In the case of a gas of which mean free path (l_{MFP}) is greater than the perforation diameter (Knudsen number, $Kn = l_{\text{MFP}}/2r > 1$), the molecular transport can be described by the free molecular flow theory. The Knudsen diffusion model known for a representative equation of the free molecular flow theory, one the other hand, is not consistent with the atomically thin porous graphene. This is because the flow impedance is determined not by diffusion inside the pores [16] but by the probability of the particles entering them. From the basic gas kinetic theory, the number of molecules hitting the exposed pore area depends on both the molecular number density, n, and their average thermal speed in one direction, or $\bar{u}/4$. Molecules on both sides of the orifice pore hit the pore area, and the net molecular flux across the membrane in thermal equilibrium is determined by the difference in n that can be related to a cross-membrane pressure difference, Δp. As the result, the molecular flow rate follows a formula of effusion:

$$\frac{Q_{\text{effusion}}}{V_{\text{m}}} = \pi r^2 \frac{\bar{u}}{4}(n_1 - n_2) = \pi r^2 \frac{\Delta p}{\sqrt{2\pi MRT}},$$

where V_{m}, M and R are the molar volume and molar mass of the transporting species and the universal gas constant, respectively.

The above equations indicate the flow rate (Q_{effusion}) across the infinitely thin filter is proportional to r^2, which means the gas flux (flow per unit pore area) is independent of the pore size in the free molecular flow region, whereas the flux in the viscous transport regime ($Q_{\text{Sampson}}/\pi r^2$) takes linear dependence on r. A well-controlled experimental characterization of nitrogen gas permeation across graphene orifices of various prescribed perforations has verified this prediction (Fig. 1).

4 Mass transfer across atomically thin orifices

4.1 Perforation on a 2D layer

The idea that an atomically thin membrane platform enables non-Fickian transport across a 2D orifice has led to endeavors to create pores in graphene on a large scale. In the early stage, high-energy electron irradiation from the transmission electron microscope (TEM) has provided means to perforate in graphene. In this way, the researchers were able to drill several holes with diameters of 3 A to 20 nm [18, 19]. Because the number of pores introduced was rather finite, this format has largely enabled characterization of DNA translocation through 2D solid-state nanopores [20, 21]. For general applications of membrane technology, it is necessary to impart more porosity to the graphene membrane.

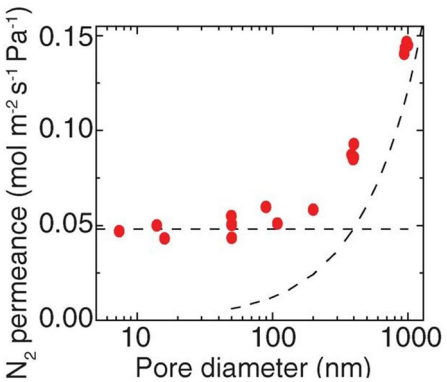

Fig. 1 Nitrogen gas permeance across atomically thin porous graphene with different pore diameters, manifesting a great asymptotic agreement with the free molecular effusion theory (horizontal dashed line) and the modified Sampson's model (dashed curve) [17]

One widespread method of obtaining a porous graphene membrane is to synthesize graphene by chemical vapor deposition (CVD). For inherent technical issues of CVD, though, as-produced polycrystalline graphene is prone to bearing defects along the grain boundaries of the crystal or sparsely distributed on the grain surface. Using such inherency, graphene can be synthesized to pose nanometer-sized pinholes ranging from 1 to 15 nm in diameter to serve as mass transport pathways across the graphene membrane [11]. These pinholes are known to be generated, if there is fine roughness, scratches or surface contamination on the catalyst, e.g., Ni or Cu, but the detailed mechanism has not been sufficiently elucidated yet.

Formation of subnanometric defects in graphene is also possible by ultraviolet-induced oxidation [22] or ozone etching [23]. Another method of creating perforations with molecular dimensions into graphene lattice is to inflict nucleation of defects through low-intensity bombardment, e.g., 8 kV, of Gallium ion followed by oxidation enlargement using acids like $KMnO_4$ and H_2SO_4.[24] Focused ion beam (FIB) can open pores from a few nanometers and to micrometer scales by striking high-energy ions (Ga^+ or He^+) on the graphene lattice [17]. In parallel, a promising top-down process for a large-scale pore generation is nanolithography, based on, for example, self-assembly of block copolymers, which can produce a mesoporous (defined by "2- to 50-nm-pored") membrane [25]. Spontaneous closure of subnanometer pores of graphene has been observed, [26] which could raise long-term stability issues of the membrane. One applicable solution has been reported in that Si atoms could block the movement of carbon atoms in graphene crystals, inhibiting the self-healing process from occurring [27]. Graphene regrowth is a notable research topic in view of both activation and protection of graphene pore edges.

5 Permeation of liquids and ions across porous graphene

5.1 Computational study on the water permeation across porous graphene

The computational results of the porous graphene-transmitted liquid flow predict a remarkable permeability of the graphene orifice to water. One molecular dynamics (MD) simulation showed ultrahigh permeability of graphene orifice [28], which can exceed that of carbon nanotubes or silicon orifices for ~2.7-nm pores. Only when the water passing through carbon nanotubes constitutes a hydrogen bond in a single row, its permeation is greater than that of graphene orifice of the same size. According to the simulation results, the pressure dropped near 1 nm away from graphene pore,

which means that most of the flow resistance occurs at the moment of incidence into pore [29].

As follows are the effects of pore size and edge that MD simulation has so far revealed [29–31]. (Prior to entering into details, note that the definitions of how to determine the size of graphene pores vary slightly in each literature. Some researchers determine the distance between ends of functional groups that suspend on the pore edge as the pore size, while others use the center of mass of carbon atoms at the edge to determine the pore size.) For pores smaller than 4 nm, the water permeability is approximately proportional to the 3.3 power of pore size, [29] which probably suggests overlapping of Sampsonian mechanics and Poiseuillian mechanics. Until present, most of the published MD simulation results are known to follow $Q \propto r^x$(x between 3 and 3.3) [28–31].

The chemical condition at graphene pore edges has an important effect on the subnanometer-sized pore region [30]. Depending on whether it is ended with hydrogen or hydroxyl group, the water permeability can be different. For sub-1-nm-wide orifice pores, it is predicted that hydrogen-ended case shows slightly less water permeability than the hydroxyl-ended case does [30]. The way to explain this phenomenon is using a polarity of water, which increases water permeability by expanding the effective pore cross section by interacting with hydroxyl group at the pore end of graphene. Researchers have extended this investigation to carboxylic-, amine- and hydroxyl-ended graphene pores to observe an intriguing configuration of water molecules within graphene's 0D confinement (Fig. 2) [33].

Another explanation is that finishing the edges of graphene orifice with hydrogen atoms makes it hydrophobic. In this way, water molecules can take a certain arranged configuration around the pore, thereby roughening the energy landscape, raising the flow resistance, and leading to decreased water permeability. In contrast, hydroxyl-ended pores can induce hydrogen bonding with water molecules and create a smooth landscape, thereby increasing overall water permeability. The research community needs more investigations to elucidate this effect.

The pore size and the edge finish can also affect the alignment of water molecules within the pore. From the spatial probability distribution of the position of water molecules, [30, 32] researchers have found out that water molecules in graphene orifice pores form themselves different from the three-dimensional counterparts do (Fig. 2). Similar to the way water molecules configure themselves inside a narrow nanotube, water molecules seem to prefer a somewhat ordered arrangement in this 0-dimensional narrow environment [30, 32].

6 Water permeation characterizations

Celebi et al. have observed the flow of water across orifices pore ranging 50 to 1000 nm made of a bilayer graphene membrane, and found that the flow only started when both sides of the orifice were pre-wetted with water [17]. If one wall was wet solely, the liquid did not pass due to capillary action, and the magnitude of capillary pressure was approximately above 2 bar. The experimentally measured water flow rate was slightly less than the Sampson flow rate quantitatively, likely caused by the pore edge effect and partly by pressurized bulging of graphene, but the function of water flux with respect to pore size followed the trend of the Sampson's flow: $Q_{H_2O} = \left(r^3/3\mu_{H_2O}\right)\Delta p$. Even when the membrane is continuously clogging, the flow rate of water measured for 50-nm pores is one magnitude greater than that of conventional ultrafiltration membranes [17]. As the pore aspect ratio increases, possible by thickening the graphene layer via atomic layer deposition (ALD), the water flux deviates from that of effusion to that of channel flows (Fig. 3) [34].

It can be challenging to measure the flow rate through the graphene orifice owing to issues such as the graphene pores clogging easily and the adhesion of graphene to porous support [17]. About the situation that the graphene tears off from the porous support, metal can be applied to the edges where the graphene meets the support to prevent graphene from being washed away by the shear stress of flow. The

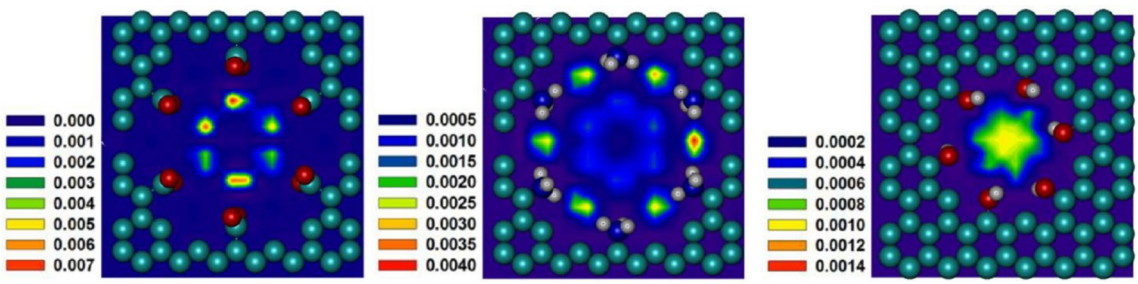

Fig. 2 Graphene pore functionalized with COO^- (left), NH_3^+ (middle), and OH^- group (right) in a weak aqueous NaCl (0.025 M). Planar density distribution indicates the density maps for oxygen atoms of water. Unit of the color contour of the atomic density is $Å^{-3}$.[33]

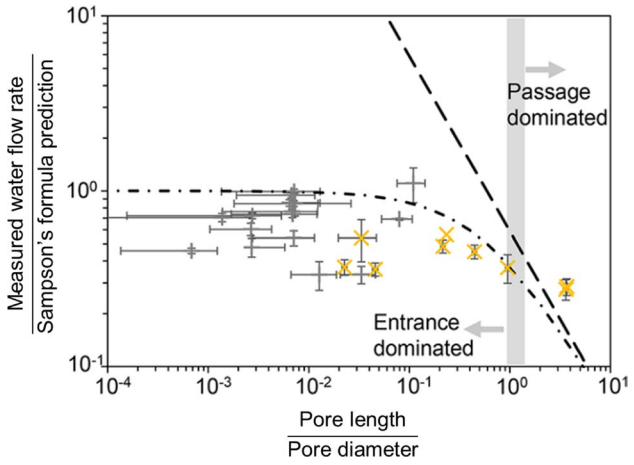

Fig. 3 Water permeation scaling of porous graphene membranes of various openings and thicknesses as a function of aspect ratio. Experimental result of water permeation is normalized by the corresponding Sampson's formula. Dagan's model (dash-dotted line) and Hagen–Poiseuille flow model (dashed line) are also normalized by Sampson's formula. As the aspect ratio decreases below 1, transport deviates from the inverse relationship of thickness–permeation because entrance-dominated resistance becomes dominant [34]

water flow data currently being measured lies somewhere between the classical Samson theory and the results of Suk and Aluru's MD simulation [29, 35]. According to Karnik et al., if ALD and interfacial polymerization cover up the defects inherent in graphene and the relatively large torn area formed during a transfer process, respectively, the single-layer substrate porous graphene can be converted into a good osmosis membrane [35]. The 0.5-nm level sub-nano pores required for this purpose were prepared with Ga^+ ion bombardment and subsequent chemical wet etching (1.875 mM $KMnO_4$ in 6.25% H_2SO_4). Despite the fact that pores are small enough to be able to filter ions out of water, the actual experimental results show that NaCl of 0.76 nm size has passed across the membrane without difficulty, and $MgSO_4$ of 0.86 nm size, Allura Red of ~1 nm size, and Dextran dyes ~3.7 nm size were only partially filtered. In other words, it was unavailable to prevent defects completely in the membrane during the study, and difficult to detect such defects thoroughly by STEM alone [35]. These results suggest how difficult to make a defect-free membrane from single-layer graphene. Moreover, this method is currently only applicable to a single layer of graphene compared to a simple physical drilling method.

Surwade et al. suggested another method of obtaining a water-permeable membrane with a single layer of graphene [36], which can produce pores by weakly treating O_2 plasma on a single layer graphene covering a 5-μm-wide opening of a SiN_x membrane. (Although it is not well explained.) In this way, pores of 1 nm size finished with Si were produced with an area density of 10^{10} cm^{-2}–10^{12} cm^{-2}.[36] However, the reported water permeation is contradictory to some degree. For example, the permeation amount driven by osmotic pressure is ~4.5×10^{-26} m^3/Pa/s per pore, which is very similar to Sampson's prediction of 6.4×10^{-26} m^3/Pa/s per pore. However, in the case of pervaporation driven by a difference in thermal energy, a device of about 20% shows a value of one digit greater than expected, for which the reason is not well known. In this experiment, the ions with low evaporation rate remain, and selectively transmit only water vapor, so that the porous graphene layer shows the possibility of seawater desalination by membrane distillation [36].

7 Ion transport through graphene nanopores

Many MD simulations predict graphene can act as a membrane that mediates selective ion transport. Simulations show that Cl^- and Br^- ion pass the hydroxyl-terminated graphene pore with ~5 Å with a mobility ratio of 17:33, while F^- or cations are blocked [37]. In contrast, graphene pore terminated by fluorine and nitrogen atoms is passed by K^+, Na^+ and Li^+ with a mobility difference of 33:14:9. Two ion separation mechanisms are conceivable from the above results: (1) electrostatic separation mechanism by a chemical group at the pore edge; (2) steric screening, which makes it easier to peel water molecules from weakly hydrated ions and pass ions through them [37].

MD simulation results from hydroxyl-terminated graphene pore are similar to natural K^+ or Na^+ channels, which indicate the usefulness of graphene as an ion separation membrane [38]. He et al. found that K^+/Na^+ selectivity ratio of pores mimicking the structure of the KcsA K^+ channel reaches 4. However, realization of Na^+-selective nanopore is more difficult. Although hydroxyl-terminated graphene pore mimics the mechanism of binding Na^+ ions to the pore edges and selectively passing ions through them, the pore size is too large to separate other types of ions [38]. Equilibrium MD simulation provides an in-depth intuition about the interaction between ions and graphene pores, for example, concentration, hydrated state and mobility of K^+ and Cl^- ions located in and around water-filled pores can be calculated [39]. The concentration of both ions(K^+, Cl^-) in the carbon-based graphene pores is less than in bulk solution (i.e., far away from graphene), which is expressed by a low partition coefficient. $\phi = c_p/c_b$, where c_p and c_b are ion concentrations in the graphene pore and the bulk reservoir, respectively. For pores smaller than 5 Å, c_p (thus ϕ) is substantially close to zero. Suk and Aluru pointed out that low ion partitioning is due to the large free energy penalty for dehydration [39], and is not consistent with the concept of dielectric exclusion of existing nanofiltration membranes [40]. In addition, it is known that the diffusion coefficient

D_p of ions in the graphene pore is lower than the diffusion coefficient D_{bulk} in solution. Correlation between D_p, D_{bulk} and pore radius r is expressed by the following equation: $\left(1/D_p - 1/D_{bulk}\right) \propto 1/r$. From this correlation, it was shown ϕ can drop to ~50%. in the 5.2 Å graphene pores [39].

Ion diffusion experiment with subnanometer-sized graphene pores has confirmed the ion selectivity based on the ion size [24]. As described above, when pores are formed on a single layer of graphene by weak ion beam irradiation followed by chemical etching, not only the pore size but also the number of pores can be controlled to some extent. In other words, pores made with very short etching time (i.e., very small pores) can result in higher permeability of cation K^+ than anion Cl^- probably due to the electrostatic charge at the pore edges. The slightly larger pores allow both K^+ and Cl^- ions to pass freely, but block dye molecules larger than the ions (e.g. Allura Red). The dye molecules pass through the pores only after sufficient etching for larger pores [24]. The study of ion permeation through subnanometer-sized pores proceeds by measuring ion conductivity [23]. Even a very weak ozone etching creates 3.8 Å size pores in graphene and allows to pass Na^+ and Cl^- ions electrodynamically. Still, it is not yet known how electrodynamics overcomes dehydration energy and passes ions, but according to a recent report by Wyss and Tian et al., the applied electric field interacts with the passing ions by adjusting the Coulomb capacity of graphene [41]. These reports provide hints on how difficult it is to fabricate nanometer-sized pores in graphene, obtain sufficient information about its size, and apply it to ion separation or selective ion permeation.

8 MD simulations to assess the applicability of porous graphene to seawater desalination

One of the promising applications for membranes with good water permeability is seawater desalination. If there is a membrane that can maintain relatively high water permeability without passing salts, the membrane may be ideal as the next generation's desalination membrane.

MD simulation, which presses a high concentration of NaCl aqueous solution to 100–225 MPa in graphene pores with a size less than 5.5 Å, confirmed 100% removal of salt. [30]

When the saline solution was pressurized to the graphene pore having a size of about 9 Å at the same magnitude, the ion selectivity was reduced depending on pressurization to 80 and 40% at 100 and 225 MPa, respectively. This result is in contrast to the phenomenon of existing reverse osmosis desalination, [42] Cohen-Tanugi and Grossman pointed out that the larger effective volume of hydrated ions, the more sensitive it is to pressure increase [30]. In addition, the effect of pore edge chemistry was remarkable. For example, pores terminated with OH-groups, which are polar moieties, allow ions to pass easily (unfavorable for water desalination). Since the OH-group at the pore edge has a similar aspect to interact with water molecules or hydrated ions, the energy barrier required for the hydrated ions to transfer into the other side can be low [30]. On the other hand, if terminated with hydrogen atoms, pores of ~8 Å show excellent desalination ability to separate 80% of ions at 100 MPa pressurization.

Equilibrium MD simulations [33] have provided information on the potential mean force (PMF) acting on water and ions around the graphene pore. Na^+ and Cl^- ions experience PMF barriers of ~0.61 and ~0.43 eV, respectively, for 7.5 Å graphene pore which have no chemical functional groups at the pore edge, while water molecules need only exceed a barrier of ~0.2 eV.[33] The simulation results predict that it is difficult to separate ions with graphene pores larger than the above. Furthermore, the size of PFM barrier is independent of salt concentration (0.025–0.25 M) for pores without chemical functional groups, but is expected to change as a function of concentration in the presence of a chemical functional group. In the case of graphene pores with a carboxylic group, the PMF for Cl^- is as high as ~0.824 eV at low concentration, but as concentration increases, it falls to ~0.47 eV since Na^+ obscures the Coulomb force from the edge of the pore. When the NH^3 moiety, which has the opposite effect of COOH moiety due to having a positive electrostatic charge, is continuously attached to the edge of pore, making the ion separation effect of two moieties is canceled, both cations and anions can penetrate the pores well [33]. Conversely, if consecutively connecting the OH^- group to the pores that retain COOH group already, it strengthens the same type of electrostatic charge, resulting in desalination of even a high-salt concentration solution such as seawater well [33].

An important property that cannot be missing in seawater desalination using perforation of graphene may be the mechanical strength of graphene membrane [43]. The pressure used in a typical reverse osmosis process is between 5 MPa (50 bar) and 10 MPa (100 bar). Because the theoretical Young's modulus of single-crystal graphene is close to 1 TPa, if making a membrane with single-crystal graphene, it will be able to withstand the mechanical pressure required for the reverse osmosis process. However, it is not yet the case and the large-scale fabrication of graphene is always accompanied by crystallographic and chemical defects. Nevertheless, according to the calculations, maintaining the porous graphene with well-selected porous support has the potential to allow the membrane endure pressures of up to about 57 MPa (570 bar) (Fig. 4) [43].

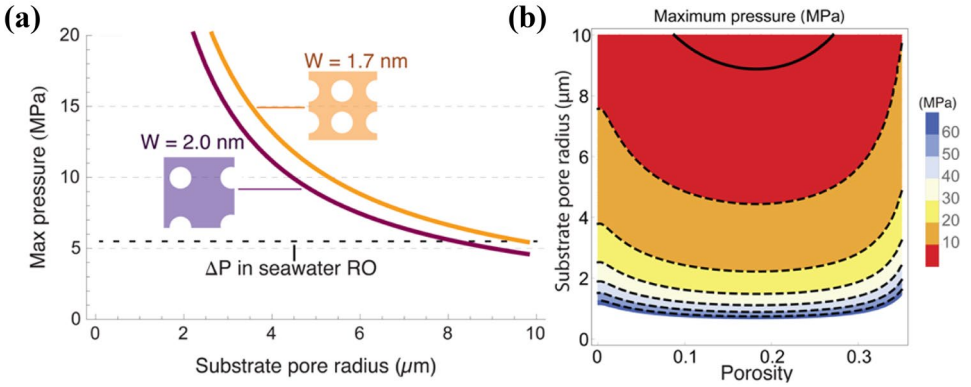

Fig. 4 **a** Failure pressure of porous graphene membrane depending on pore size. Porous graphene membranes with various pore radius mostly withstand higher pressures than conventional seawater RO. At the same pore radius, porous graphene with a small W (nanopore separation length) is more resistant to pressure than a larger one. **b** Contour plot of maximum pressure of nanoporous graphene membrane as a function of pore radius and porosity [43]

9 Mass transport properties in graphene oxide lamellar membrane

9.1 Selective permeation of gases

While the perforation on impermeable 2D material can create molecular transport pathways through nanometer-scale pores, staggered stacking of platelets of 2D material can also engender an interesting architecture for nanoscale transport pathways. Graphene platelets produced in various methods end up posing a mixed configuration of pristine and chemically modified graphene regions. Ideally, stacked lamellae of pristine graphene by van der Waals interaction have an interlayer spacing of ~3.4 Å, unsuitable for a mass transfer pathway. However, graphene oxide (GO) platelets, chemically derived from graphene, can construct molecular-scale columns and spacers in their interlayer space during stacking to create pathways for permeation. Although it might not be easy, as long as the interlayer spacing of GO platelets were controlled, innovations in various chemical separation technologies would come true.

It has been reported that the permeation rate of water vapor through thick GO lamellae (0.1–10 μm) is comparable to that of evaporation from an open-water surface under similar conditions (Fig. 5a). In addition, GO membrane exhibited high selectivity for water by preventing the permeation of He molecules despite smaller molecular size than that of water. From this observation, we realize that the nanochannels formed in between the GO platelets can transfer water selectively by their strong interaction with water molecules (Fig. 5b) [44]. This report has sparked widespread interest in the research and development of the GO membrane due to its excellent selectivity for water and easy preparation of samples. Perhaps the most important factor affecting the gas permeability and selectivity of GO membrane is the stacking

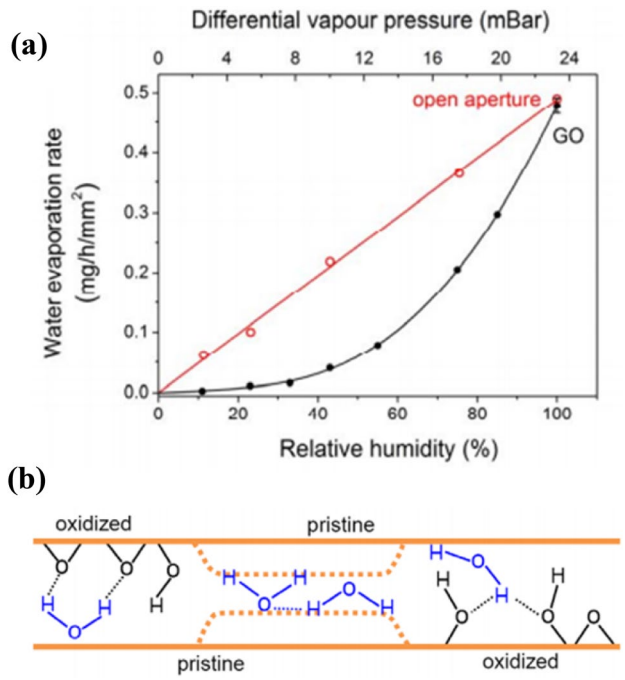

Fig. 5 **a** Permeation rate of water vapor through open aperture (without GO membrane) and GO membrane. As the relative humidity increases, the water permeation rates of GO membrane approximate that of the open aperture, and show little difference at 100% RH. **b** Schematic illustration of nanochannels formed between two adjacent GO nanosheets. Water can transport fast due to the interaction of the oxidized region with water molecules, and the water path provided by the pristine graphene channel [44]

method of 2D platelets and the strategy of interlocking layers. In particular, the selectivity of GO membrane for gas species can be roughly explained by the kinetic diameter (Fig. 6), which may lead to a molecular sieving mechanism. However, the permeability of some gases deviates from the

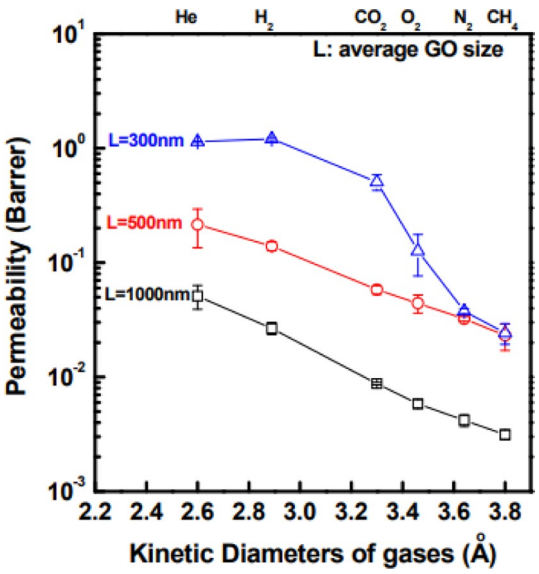

Fig. 6 Gas permeabilities of graphene oxide membrane with different kinetic diameters of gases. Gas permeabilities generally decrease with increasing kinetic diameter. Changing the size of graphene oxide sheets (300, 500, and 1000 nm) affects gas transport, and thus gas permeabilities tend to increase as the size decreases [45]

kinetic diameter theory, calling for further elucidation [45, 46].

10 Selective permeation of water

A typical way of producing a GO lamellar membrane for nanofiltration is to stack colloidal GO platelets with lateral dimension ranging between tens of nanometer and several micrometers on a filter support out of anodic aluminum oxide (AAO). Although they reject merely <60% of relatively small ions, such as NaCl, Na_2SO_4, $MgCl_2$ and $MgSO_4$, the inter-GO-layer nanochannels can filter out most of such large molecules such as methyl blue and direct red 81 without significant loss of water permeation rate that is often higher than those of commercial polymeric nanofiltration membranes (Table 1). These successful charged-dye retention results are attributed to both Gibbs–Donna equilibrium theory (electrostatic interaction) [47] and hindrance transport theory (size exclusion).

It is known that the GO lamella is vulnerable in an aqueous environment, for thermodynamics favors GO flakes to be dispersed in water, which raises a concern on the long-term stability of the GO membrane for water purification applications [48]. As one cure for the membrane disintegration, polydopamine has been used to bridge GO flakes. Chemical bonding in between GO flakes could be formed using 1,3,5-benzenetricarbonyl trichloride, resulting in 8–27.6 L m^{-2} h^{-1} bar^{-1}. The retention for large organic molecules is higher (> ~ 93% for Rodamine-WT) than for small ions (6–19% for NaCl), hinting adaptability of the GO membrane to nanofiltration. It is interesting that both water flux and salt rejection do not depend strongly on the number of GO layers or thickness of the lamellar GO membrane (Fig. 7). According to this finding, even a very thin GO membrane could, in principle, separate ions and organic matters in water. An additional fact that the ion rejection lowers with ion concentration confirms the action of the charge-based exclusion mechanism by way of Debye length shortening [49].

In contrast to previous reports, if GO is placed on alumina filters during vacuum filtration, membranes maintained great stability in water without any interlayer bonding agent. The micrometer-thick GO membranes prepared in this way have shown selective transport towards water only, a similar result to water vapor transport across GO membranes of similar thicknesses. Ions with large hydrated radii can be separated via size exclusion. Charge of ions or molecules, however, did not play a decisive role in the separation, which is supported by an observation that permeation rate of AsO_4^{3-} was almost identical to that of Na^+ or Cl^- (Fig. 8) [50]. This observation hints that electrostatic interaction may get much weakened in the so-called charge-neutralized environment caused by the insertion of aluminum cations in the interspace of GO platelets.

Forward osmosis (FO) is another water technology application of the stacked 2D membranes. For an FO process,

Table 1 Retention of organic dyes for ultrathin graphene nanofiltration membranes with different base-refluxing-reduced GO (brGO) loadings and brGO layer thickness [47].

brGO loading [mg m^{-2}]	Thickness [nm]	Pure water flux J_0 [L $m^{-2}h^{-1}$ bar^{-1}]	MB[a]			DR 81[a]		
			Retention [%]	J/J_0 [%][b]	C/C_0[c]	Retention [%]	J/J_0 [%][b]	C/C_0[c]
14.1[d]	22	21.81	99.2	90.0	1.27	99.9	89.6	1.31
17.0[e]	26	12.62	99.7	91.1	1.30	99.8	89.7	1.33
21.2[e]	33	5.00	99.7	89.4	1.32	99.9	87.2	1.33
28.3[e]	44	4.37	99.6	90.4	1.33	99.9	95.8	1.34
34.0[e]	53	3.26	99.8	95.0	1.36	99.9	95.6	1.35

[a]The concentration of feed dye solution C_0 was 0.02 mM. [b]The ratio of permeate flux of the dye solution J to the pure water flux J_0. [c] Concentration ratio of upper stream (C) when the permeation volume was 10 mL to the original feeding solution (C_0, 35 mL). [d]The applied pressure was 1 bar. [e]The applied pressure was 5 bar.

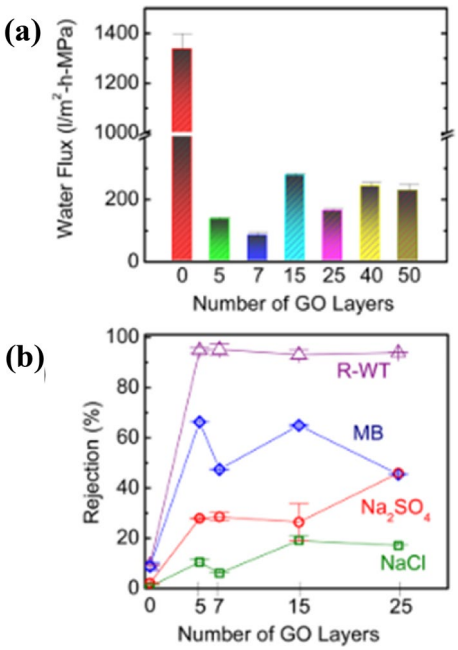

Fig. 7 **a** Water flux and **b** rejection (salts, organic dyes) of graphene oxide membrane with changing the number of layers [49]

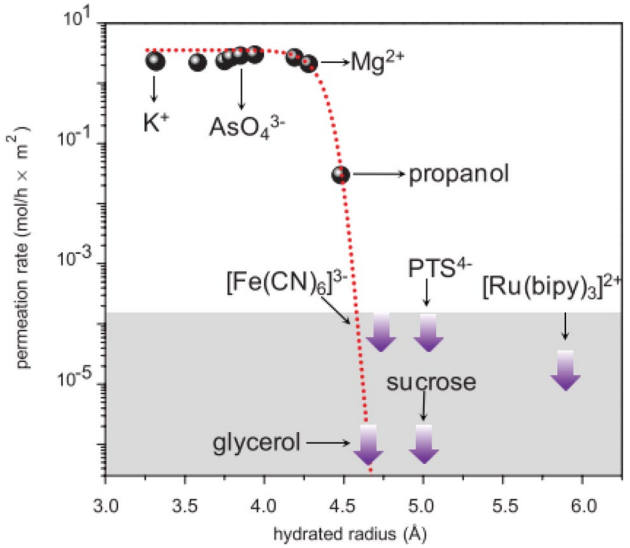

Fig. 8 Permeation rates of various ionic and molecular species through 5-μm-thick graphene oxide membrane. Unlike species with small hydrated radius (<4.5 Å), the permeation rate of large species (>4.5 Å) is negligibly low (gray area), suggesting size-dependent selectivity [50]

a freestanding reduced GO (rGO) membrane has shown a promising result. Freestanding rGO membranes show high permeance (57.0 L m^{-2} h^{-1} when DI water and NaCl (2.0 M) were used as feed and draw solutions, respectively) than a commercial FO membrane (CTA membrane, ~10 L m^{-2} h^{-1} at the same conditions). This finding is particularly important because freestanding rGO membranes could eliminate the most problematic issue of an internal concentration polarization of the FO process, leading to an increase in the effective chemical potential difference. Importantly, the reverse salt flux (from draw to feed) in g m^{-2} h^{-1} is lower for this membrane, and so the salt rejection capability of rGO membranes is greater than that of CTA [51].

11 Theoretical investigations

Through simulation, it is possible to explain the superior performance of the layered graphene structure, which is difficult to identify by experiment alone, as well as to predict an unseen phenomenon. Using first-principle simulation, researchers have found out that the minimum resistance flow between two adjacent graphene sheets is related to a unique two-dimensional hydrogen bond structure formed between water molecules. Unlike the one-dimensional narrow space inside the CNT, the average number of hydrogen bonds per water molecule does not change much in the two-dimensional space, even if the narrow space size is about 10 Å. In addition, since the perturbation of hydrogen bonds is mainly limited to the symmetrical interface where graphene and water molecules meet, the tendency of water molecules to tilt toward graphene along with the dipole moment of water molecules is weakened. As the result, water mobility can be augmented, in theory, in the two-dimensional narrow space [52].

On the other hand, the phenomenon that water appears to transform the phase from liquid to solid in the narrow space supports anomalous transport of water in a two-dimensional space. In contrast to He, Ar, N_2, H_2, etc., only hydrogen-bonded water can phase-transform in an extremely narrow graphene channel. According to this theory, since ice having a long-range order in a two-dimensional narrow space is energetically preferred than the liquid phase, water would configure the ice structure to instigate collective motion and effectively reduced flow resistance. According to the simulation results, when the two-dimensional channel between graphene sheets gets slightly wider (7–10 Å), bilayer of 2D ice is formed, resulting in lower thermodynamic energy [53].

Molecular-level slip flow has been theoretically predicted within the graphene channel. Due to the slippery and crystalline nature of graphene, molecules tend to slip over the surface of graphene. Over the entire range of fluid flows, the slip length of water on graphene is much longer than the other chemical species such as Ar and CH_4. The slip lengths of liquid phase Ar, CH_4 and water are reported to be 11 ± 1 nm, 5.9 ± 0.6 nm and 60 ± 6 nm, respectively [54].

Layered graphene structure exhibits the minimum resistance flow of water and its high degree of separation

compared to other species is a collaboration of nanometer-level tight stricture, physical properties of graphene, and unique physical and transport properties of water formed in the narrow space. Therefore, the lamellar architecture poses excellent potential to use in basic scientific research and engineering applications including membrane technology.

12 Conclusions

Achieving great permeance while maintaining high selectivity has been considered a must-solve goal in the separation technology, despite being considered to overcome the challenging problem of selectivity–permeance trade-off limits. Porous graphene, a membrane out of perforated freestanding graphene, does not only exhibit excellent mechanical and chemical stability but also shows the ultimate permeation. Theoretically, porous graphene with subnanometer pore size and high areal porosity is considered a material that will revolutionize the separation industry, such as water purification and seawater desalination. The unique edge chemistry of orifices (or pores) in porous graphene contributes significantly to improving selectivity and even affects water permeance. Recently, in addition, lamellar membranes comprising two-dimensional graphene or oxidized graphene sheets have been produced through various methods, e.g., pressurized vacuum filtering, layer-by-layer stacking, spin-coating, etc., with providing selectivity for partitioning target species from water. The selectivity of the stacked-graphene oxide membrane is largely reliant on electrostatic interaction and size exclusion, thus separation performance can be changed by modulating the structure and chemical properties of the membrane, e.g., interlayer spacing and surface charge.

The unique structure and properties of porous 2D sheets and stacked platelets are expected to have the potential to realize ultimate permeance with high selectivity. After understanding the characteristics of these two structures in depth, it is possible to design an optimal membrane structure that is practical in water treatment and other separation research fields. Consequently, experiments and simulations are needed to understand the properties and fundamental mass transport mechanisms of nanomaterials that have not yet been identified. In addition, research toward ingenious engineering of membrane manufacturing that enables large-scale, low-price and rapid production can increase the possibility of approaching practical applications.

Acknowledgements This work was supported by the National Research Foundation of Korea (NRF) grant funded by the Korea government (MSIT) (No. 2020R1A3B2079741). A part of this work was supported by KOREA HYDRO & NUCLEAR POWER CO., LTD (No. 2019-TECH-17).

Compliance with ethical standards

Conflict of interest All the authors claim no conflict of interest.

References

1. K.S. Novoselov, A.K. Geim, S.V. Morozov, D. Jiang, Y. Zhang, S.V. Dubonos, I.V. Grigorieva, A.A. Firsov, Electric field effect in atomically thin carbon films. Science **306**, 666–669 (2004)
2. O. Leenaerts, B. Partoens, F.M. Peeters, Graphene: a perfect nanoballoon. Appl. Phys. Lett. **93**, 193107 (2008)
3. J.S. Bunch, S.S. Verbridge, J.S. Alden, A.M. Van Der Zande, J.M. Parpia, H.G. Craighead, P.L. McEuen, Impermeable atomic membranes from graphene sheets. Nano Lett. **8**, 2458–2462 (2008)
4. T. Georgiou, L. Britnell, P. Blake, R.V. Gorbachev, A. Gholinia, A.K. Geim, C. Casiraghi, K.S. Novoselov, Graphene bubbles with controllable curvature. Appl. Phys. Lett. **99**, 093103 (2011)
5. L. Tsetseris, S.T. Pantelides, Graphene: an impermeable or selectively permeable membrane for atomic species? Carbon **67**, 58–63 (2014)
6. V. Berry, Impermeability of graphene and its applications. Carbon **62**, 1–10 (2013)
7. O. Lehtinen, J. Kotakoski, A.V. Krasheninnikov, A. Tolvanen, K. Nordlund, J. Keinonen, Effects of ion bombardment on a two-dimensional target: atomistic simulations of graphene irradiation. Phys. Rev. B Condens. Matter Mater. Phys. **81**, 153401 (2010)
8. S. Hu, M. Lozada-Hidalgo, F.C. Wang, A. Mishchenko, F. Schedin, R.R. Nair, E.W. Hill, D.W. Boukhvalov, M.I. Katsnelson, R.A. Dryfe, I.V. Grigorieva, H.A. Wu, A.K. Geim, Proton transport through one-atom-thick crystals. Nature **516**, 227–230 (2014)
9. S. Chen, L. Brown, M. Levendorf, W. Cai, S.-Y. Ju, J. Edgeworth, X. Li, C.W. Magnuson, A. Velamakanni, R.D. Piner, J. Kang, J. Park, R.S. Ruoff, Oxidation resistance of graphene-coated Cu and Cu/Ni alloy. ACS Nano **5**, 1321–1327 (2011)
10. Y.-P. Hsieh, M. Hofmann, K.-W. Chang, J.G. Jhu, Y.-Y. Li, K.Y. Chen, C.C. Yang, W.-S. Chang, L.-C. Chen, Complete corrosion inhibition through graphene defect passivation. ACS Nano **8**, 443–448 (2014)
11. S.C. O'Hern, C.A. Stewart, M.S.H. Boutilier, J.-C. Idrobo, S. Bhaviripudi, S.K. Das, J. Kong, T. Laoui, M. Atieh, R. Karnik, Selective molecular transport through intrinsic defects in a single layer of CVD graphene. ACS Nano **6**, 10130–10138 (2012)
12. T. Yoon, J.H. Mun, B.J. Cho, T.S. Kim, Penetration and lateral diffusion characteristics of polycrystalline graphene barriers. Nanoscale **6**, 151–156 (2014)
13. M. Schriver, W. Regan, W.J. Gannett, A.M. Zaniewski, M.F. Crommie, A. Zettl, Graphene as a long-term metal oxidation barrier: worse than nothing. ACS Nano **7**, 5763–5768 (2013)

14. R.A. Sampson, On Stokes's current function. Philos. Trans. R. Soc. Lond. A **182**, 449–518 (1891)
15. K.-K. Tio, S.S. Sadhal, Boundary conditions for stokes flows near a porous membrane. Appl. Sci. Res. **52**, 1–20 (1994)
16. M. Knudsen, Die Molekularströmung der Gase durch Offnungen und die Effusion. Ann. Phys. **333**, 999–1016 (1909)
17. K. Celebi, J. Buchheim, R.M. Wyss, A. Droudian, P. Gasser, I. Shorubalko, J.I. Kye, C. Lee, H.G. Park, Ultimate permeation across atomically thin porous graphene. Science **344**, 289–292 (2014)
18. M.D. Fischbein, M. Drndić, Electron beam nanosculpting of suspended graphene sheets. Appl. Phys. Lett. **93**, 113107 (2008)
19. C.J. Russo, J.A. Golovchenko, Atom-by-atom nucleation and growth of graphene nanopores. Proc. Natl. Acad. Sci. USA **109**, 5953–5957 (2012)
20. C.A. Merchant, K. Healy, M. Wanunu, V. Ray, N. Peterman, J. Bartel, M.D. Fischbein, K. Venta, Z. Luo, A.T.C. Johnson, M. Drndic, DNA translocation through graphene nanopores. Nano Lett. **10**, 2915–2921 (2010)
21. G.G.F. Schneider, S.W. Kowalczyk, V.E. Calado, G.G. Pandraud, H.W. Zandbergen, L.M.K. Vandersypen, C. Dekker, DNA translocation through graphene nanopores. Nano Lett. **10**, 3163–3167 (2010)
22. S.P. Koenig, L. Wang, J. Pellegrino, J.S. Bunch, Selective molecular sieving through porous graphene. Nat. Nanotechnol. **7**, 728–732 (2012)
23. M.I. Walker, R.S. Weatherup, N.A.W. Bell, S. Hofmann, U.F. Keyser, Free-standing graphene membranes on glass nanopores for ionic current measurements. Appl. Phys. Lett. **106**, 023119 (2015)
24. S.C. O'Hern, M.S. Boutilier, J.C. Idrobo, Y. Song, J. Kong, T. Laoui, M. Atieh, R. Karnik, Selective ionic transport through tunable subnanometer pores in single-layer graphene membranes. Nano Lett. **14**, 1234–1241 (2014)
25. J. Bai, X. Zhong, S. Jiang, Y. Huang, X. Duan, Graphene nanomesh. Nat. Nanotechnol. **5**, 190–194 (2010)
26. R. Zan, Q.M. Ramasse, U. Bangert, K.S. Novoselov, Graphene reknits its holes. Nano Lett. **12**, 3936–3940 (2012)
27. J. Lee, Z. Yang, W. Zhou, S.J. Pennycook, S.T. Pantelides, M.F. Chisholm, Stabilization of graphene nanopore. Proc. Natl. Acad. Sci. USA **111**, 7522–7526 (2014)
28. M.E. Suk, N.R. Aluru, Water transport through ultrathin graphene. J. Phys. Chem. Lett. **1**, 1590–1594 (2010)
29. M.E. Suk, N.R. Aluru, Molecular and continuum hydrodynamics in graphene nanopores. RSC Adv. **3**, 9365–9372 (2013)
30. D. Cohen-Tanugi, J.C. Grossman, Water desalination across nanoporous graphene. Nano Lett. **12**, 3602–3608 (2012)
31. D. Zhou, Y. Cui, P.W. Xiao, M.Y. Jiang, B.H. Han, A general and scalable synthesis approach to porous graphene. Nat. Commun. **5**, 4716 (2014)
32. C. Zhu, H. Li, S. Meng, Transport behavior of water molecules through two-dimensional nanopores. J. Chem. Phys. **141**, 18C528 (2014)
33. D. Konatham, J. Yu, T.A. Ho, A. Striolo, Simulation insights for graphene-based water desalination membranes. Langmuir **29**, 11884–11897 (2013)
34. J. Buchheim, K.P. Schlichting, R.M. Wyss, H.G. Park, Assessing the thickness-permeation paradigm in nanoporous membranes. ACS Nano **13**, 134–142 (2019)
35. S.C. O'Hern, D. Jang, S. Bose, J.C. Idrobo, Y. Song, T. Laoui, J. Kong, R. Karnik, Nanofiltration across defect-sealed nanoporous monolayer graphene. Nano Lett. **15**, 3254–3260 (2015)
36. S.P. Surwade, S.N. Smirnov, I.V. Vlassiouk, R.R. Unocic, G.M. Veith, S. Dai, S.M. Mahurin, Water desalination using nanoporous single-layer graphene. Nat. Nanotechnol. **10**, 459–464 (2015)
37. K. Sint, B. Wang, P. Král, Selective ion passage through functionalized graphene nanopores. J. Am. Chem. Soc. **130**, 16448–16449 (2008)
38. Z. He, J. Zhou, X. Lu, B. Corry, Bioinspired graphene nanopores with voltage-tunable ion selectivity for Na^+ and K^+. ACS Nano **7**, 10148–10157 (2013)
39. M.E. Suk, N.R. Aluru, Ion transport in sub-5-nm graphene nanopores. J. Chem. Phys. **140**, 084707 (2014)
40. A.E. Yaroshchuk, Dielectric exclusion of ions from membranes. Adv. Colloid Interfaces **85**, 193–230 (2000)
41. R.M. Wyss, T. Tian, K. Yazda, H.G. Park, C.J. Shih, Macroscopic salt rejection through electrostatically gated nanoporous graphene. Nano Lett. **19**, 6400–6409 (2019)
42. M.E. Williams, A review of reverse osmosis theory. in, EET Corporation and Williams Engineering Services Company Inc (2003).
43. D. Cohen-Tanugi, J.C. Grossman, Mechanical strength of nanoporous graphene as a desalination membrane. Nano Lett. **14**, 6171–6178 (2014)
44. R.R. Nair, H.A. Wu, P.N. Jayaram, I.V. Grigorieva, A.K. Geim, Unimpeded permeation of water through helium-leak-tight graphene-based membranes. Science **335**, 442–444 (2012)
45. H.W. Kim, H.W. Yoon, S.M. Yoon, B.M. Yoo, B.K. Ahn, Y.H. Cho, H.J. Shin, H. Yang, U. Paik, S. Kwon, J.Y. Choi, H.B. Park, Selective gas transport through few-layered graphene and graphene oxide membranes. Science **342**, 91–95 (2013)
46. H. Li, Z. Song, X. Zhang, Y. Huang, S. Li, Y. Mao, H.J. Ploehn, Y. Bao, M. Yu, Ultrathin, molecular-sieving graphene oxide membranes for selective hydrogen separation. Science **342**, 95–98 (2013)
47. Y. Han, Z. Xu, C. Gao, Ultrathin graphene nanofiltration membrane for water purification. Adv. Funct. Mater. **23**, 3693–3700 (2013)
48. C.N. Yeh, K. Raidongia, J.J. Shao, Q.H. Yang, J.X. Huang, On the origin of the stability of graphene oxide membranes in water. Nat. Chem. **7**, 166–170 (2015)
49. M. Hu, B. Mi, Enabling graphene oxide nanosheets as water separation membranes. Environ. Sci. Technol. **47**, 3715–3723 (2013)
50. R.K. Joshi, P. Carbone, F.C. Wang, V.G. Kravets, Y. Su, I.V. Grigorieva, H.A. Wu, A.K. Geim, R.R. Nair, Precise and ultrafast molecular sieving through graphene oxide membranes. Science **343**, 752–754 (2014)
51. H. Liu, H. Wang, X. Zhang, Facile fabrication of freestanding ultrathin reduced graphene oxide membranes for water purification. Adv. Mater. **27**, 249–254 (2015)
52. G. Cicero, J.C. Grossman, E. Schwegler, F. Gygi, G. Galli, Water confined in nanotubes and between graphene sheets: a first principle study. J. Am. Chem. Soc. **130**, 1871–1878 (2008)
53. D.W. Boukhvalov, M.I. Katsnelson, Y.W. Son, Origin of anomalous water permeation through graphene oxide membrane. Nano Lett. **13**, 3930–3935 (2013)
54. S.K. Kannam, B.D. Todd, J.S. Hansen, P.J. Daivis, Slip flow in graphene nanochannels. J. Chem. Phys. **135**, 144701 (2011)

Heechan Yang is currently a doctoral student at Pohang University of Science and Technology (POSTECH), Pohang, Korea, under the supervision of Prof. Hyung Gyu Park. He received his B.S. degree in Mechanical Engineering from Kyung Hee University, in 2019. His research interest includes low-dimensional fluidics, two-dimensional lamellar structure, and their applications in membrane technology and sustainable energy.

Jonghyun Baek is currently a doctoral student at Pohang University of Science and Technology (POSTECH), Pohang, Korea, under the supervision of Prof. Hyung Gyu Park. He received his B.S. degree in Mechanical Engineering from Hanyang University, in 2019. His research interest lies at nanofluidics across 2D materials and their applications for energy sustainability through plasmonic catalysis.

Hyung Gyu Park is a Full Professor in the Department of Mechanical Engineering at Pohang University of Science and Technology (POSTECH), Pohang, Korea. He received his PhD in Mechanical Engineering from the University of California, Berkeley, in 2007, with pioneering research on nanoscale mass transport inside carbon nanotubes in collaboration with Lawrence Livermore National Laboratory (LLNL). After postdoctoral research at LLNL, he embarked on his independent research career as an assistant professor at Swiss Federal Institute of Technology (ETH) Zurich, Switzerland, in 2009, which awarded him a tenure position in 2015. He joined POSTECH in 2019 and continues to lead the laboratory of Nanoscience for Energy Technology and Sustainability. His research interest spans from carbon nanomaterials syntheses and surface enhanced Raman spectroscopy to low-dimensional fluidics and process intensification with membrane science.

Affiliations

Heechan Yang[1] · Jonghyun Baek[1] · Hyung Gyu Park[1]

[1] Nanoscience for Energy Technology and Sustainability, Department of Mechanical Engineering, Pohang University of Science and Technology (POSTECH), Pohang 37673, Gyeongbuk, Korea